Plasmas Computed with ATMED CR of the 4th Non-LTE Code Comparison Workshop Database

In this paper, there are presented some results calculated with ATMED CR of the 4th Non-LTE Code Comparison Workshop held in December 2005, when this software didn't exist, having been released in 2017. NLTE population kinetics codes were tested of steady-state cases for C, Ar, Fe, Sn, Xe and Au plasmas selected for detailed comparisons. Apart from analyzing dense plasma physics, the scope was expanded including the EUV lithography sources and photoionized plasmas.

The results for plasma properties can be considered as relatively precise and optimal, being checked fundamentally the high sensitivity of calculations to changes in regime, local thermodynamic equilibrium (LTE) or non-LTE (NLTE), electronic and radiation temperatures, electronic density and plasma length. Frequency resolved and mean opacities are also displayed computed with ATMED CR using UTA (Unresolved Transition Array) formalism.

Keywords:

Screened Hydrogenic Atomic Model; Collisional Radiative Average Atom Code; Plasmas of NLTE-4 Workshop

1. INTRODUCTION

The collisional radiative model ATMED CR [1,2] constructed in the Average Atom formalism has been developed to calculate plasma population kinetics under coronal, local or non-local thermodynamic equilibrium regimes as an extension of the module named ATMED LTE [3-5] designed previously for local thermodynamic conditions. The atomic model is based on a New Relativistic Screened Hydrogenic Model (NRSHM) with a set of universal screening constants including *nlj*-splitting that has been obtained by fitting to a large database of 61,350 atomic high quality data entries, compiled from the National Institute of Standards and Technology (NIST) database of U.S. Department of Commerce and from the Flexible Atomic Code (FAC) [6,7].

The calculation of accurate relativistic atomic populations including *nlj*-splitting of electronic orbitals, improves the precision of atomic properties as mean charge, rates and the resolution of spectral properties as opacities and radiative power losses, with respect to collisional radiative average atom codes as XSN of W. Lokke and W. Grasberger of 1977 with *n*-splitting [8,9] or considering *nl*-splitting [10-13]. The CR balance is based on iterative loops for reaching auto convergence in populations and plasma mean charge [14]. The accuracy ATMED CR code can achieve can be consulted in Section 3 of Ref. [15] which explains in detail the phases of the investigation project, consisting of the comparison of plasma properties of this software with bibliographic data.

The implementation of the collisional radiative balance with the new atomic model, allows now to compute plasmas in NLTE regime or coronal regime, widening considerably for all chemical elements the validity range of thermodynamic conditions [16,17]. In Section 2 there are modeled plasmas with ATMED CR illustrating the high agreement with results for plasma properties of other codes. Section 3 contains main conclusions. Details about the workshop, motivations for the chosen cases and discussion of some representative results can be found in References [18-20].

2. PLASMAS OF 4TH NLTE DATABASE

The problems proposed for the steady-state cases of C, Ar, Sn, Xe and Au atoms have been calculated with the collisional radiative average atom code ATMED CR. Some graphs are displayed by courtesy of the database (https://nlte.nist.gov/NLTE4/) for visual comparison of plasma properties.

2.1 Carbon Plasmas

The following problems have been established for the steady-state cases of carbon atoms on a grid of electron temperatures and electron densities, see Table 1 and Figure 1:

Element	Case ID	Total # of Points	Parameter	Grid	# of Points
Detailed NLTE case (proposed at NLTE-3); comparison with the benchmark theoretical results					
Carbon	C	16	T_e	3, 5, 7, 10	4
			N_e	10^{13}, 10^{15}, 10^{17}, 10^{19}	4

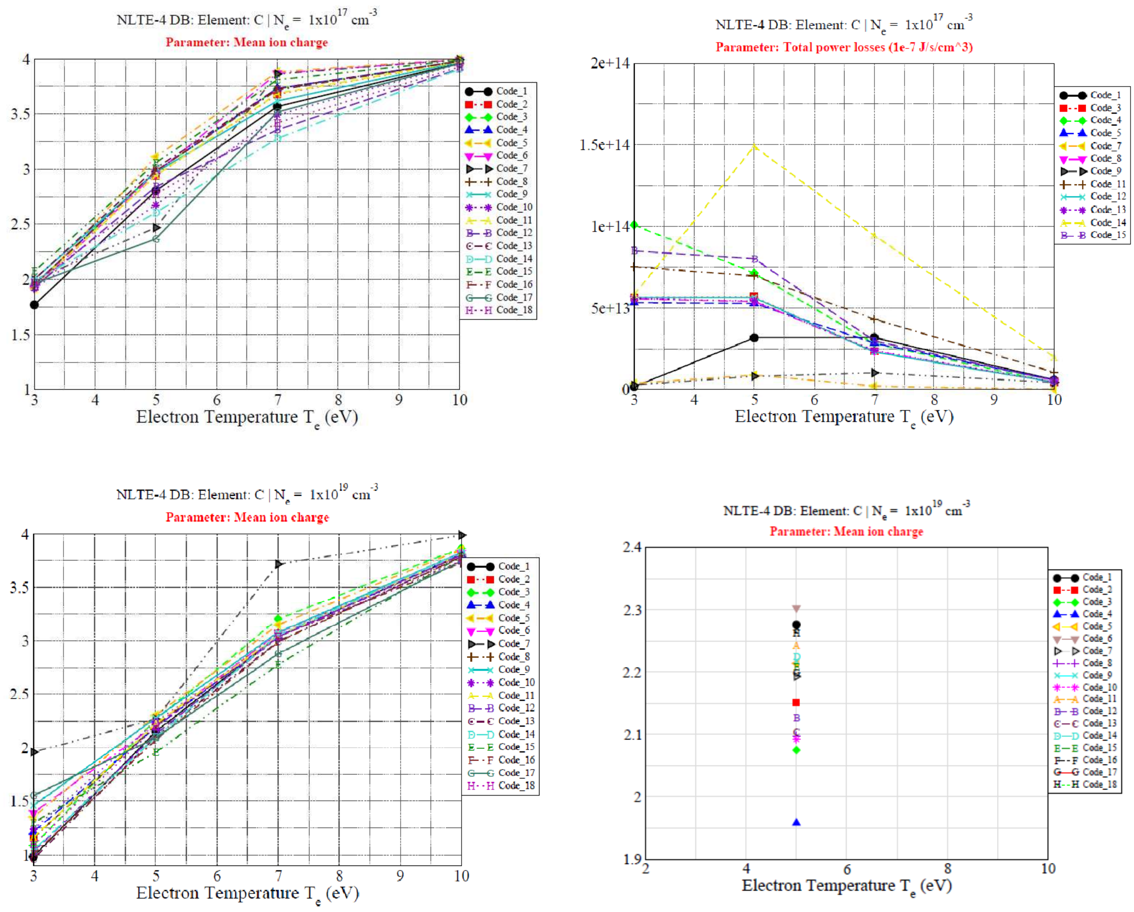

Figure 1.a. Carbon plasma properties computed with participant codes of NLTE-4 Workshop

In Figure 1 and Table 1 there are displayed values of carbon plasmas, checking the high agreement of ATMED CR results with respect to other participant codes, being as well as a snapshot of the high sensitivity to slight changes in temperatures or densities. In tables there are indicated the approximated ranges of mean charge for all plasma cases.

Table 1: Carbon plasma properties of ATMED CR for comparison with codes of NLTE-4 Workshop

N_e (cm^{-3}) = 10^{13}	ρ (g/cm^3)	Z_{bar} ATMED	Z_{bar} NLTE-4	η_e ATMED CR	K_R (cm^2/g)	K_P (cm^2/g)	RPL (1e-7 J/cm^3/s)
T_e = 3 eV	1.040E-10	1.926E+00	1.2÷2	-2.1862E+01	1.557E+01	2.638E+04	3.938131E+03
T_e = 10 eV	1.015E-10	1.981E+00	3.2÷4	-2.3664E+01	1.157E+02	3.219E+05	2.521072E+05
N_e (cm^{-3}) = 10^{15}	**ρ (g/cm^3)**	**Z_{bar} ATMED**	**Z_{bar} NLTE-4**	**η_e ATMED CR**	**K_R (cm^2/g)**	**K_P (cm^2/g)**	**RPL (1e-7 J/cm^3/s)**
T_e = 3 eV	1.450E-08	1.953E+00	1.4÷2	-1.6911E+01	6.540E+01	2.485E+04	4.820444E+07
T_e = 5 eV	1.500E-08	1.958E+00	1.8÷2.9	-1.7641E+01	2.830E+02	2.008E+05	4.504697E+08
T_e = 7 eV	9.000E-09	2.247E+00	2.2÷3.7	-1.8518E+01	9.876E+02	2.561E+05	7.903052E+08
T_e = 10 eV	5.150E-09	3.897E+00	3.3÷4	-1.9061E+01	3.811E+01	4.609E+03	2.035248E+09
N_e (cm^{-3}) = 10^{17}	**ρ (g/cm^3)**	**Z_{bar} ATMED**	**Z_{bar} NLTE-4**	**η_e ATMED CR**	**K_R (cm^2/g)**	**K_P (cm^2/g)**	**RPL (1e-7 J/cm^3/s)**
T_e = 5 eV	6.200E-07	3.222E+00	2.4÷3.2	-1.3421E+01	3.684E+04	7.617E+04	2.160765E+12
T_e = 7 eV	6.000E-07	3.445E+00	3.3÷3.9	-1.3892E+01	2.530E+04	3.836E+04	3.487695E+12
T_e = 10 eV	5.300E-07	3.830E+00	3.8÷4	-1.4445E+01	7.957E+02	1.192E+04	1.628114E+12
N_e (cm^{-3}) = 10^{19}	**ρ (g/cm^3)**	**Z_{bar} ATMED**	**Z_{bar} NLTE-4**	**η_e ATMED CR**	**K_R (cm^2/g)**	**K_P (cm^2/g)**	**RPL (1e-7 J/cm^3/s)**
T_e = 5 eV	9.000E-05	2.330E+00	2÷2.3	-8.7669E+00	4.637E+04	2.032E+05	2.427511E+13
T_e = 7 eV	6.100E-05	3.278E+00	2.8÷3.2	-9.3195E+00	4.005E+04	5.318E+04	1.181351E+13
T_e = 10 eV	5.300E-05	3.853E+00	3.7÷4	-9.8334E+00	2.367E+03	1.138E+04	6.402962E+12

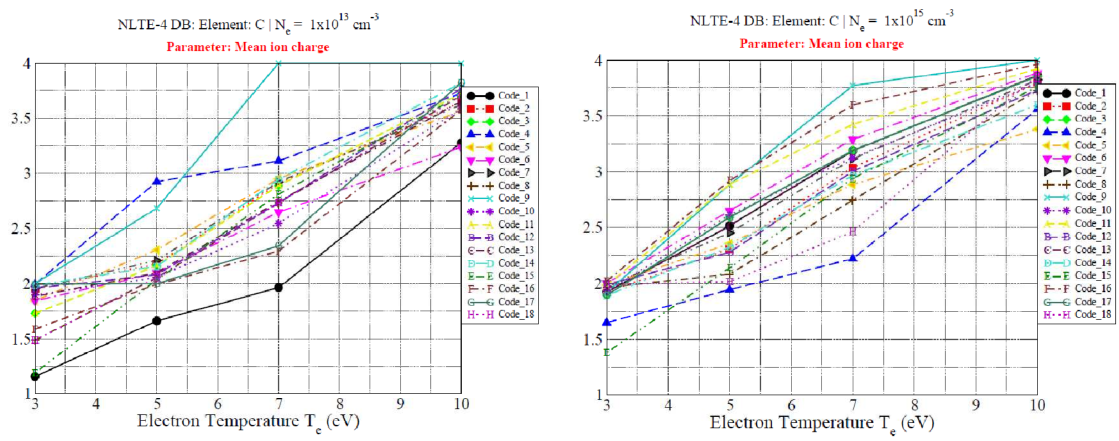

Figure 1.b. Carbon plasma properties computed with participant codes of NLTE-4 Workshop

2.2 Argon Plasmas

The following problems have been established for the steady-state cases of argon atoms on a grid of electron temperatures and electron densities, see Table 2 and Figure 2:

Element	Case ID	Total # of Points	Parameter	Grid	# of Points
The same case (almost) as in NLTE-3; non-Maxwellian; **test the progress since NLTE-3**					
Argon	Ar	24	T_e	50, 100, 300, 600	4
			N_e	10^{12}, 10^{18}, 10^{23}	3
			T_2	10^4 (10 keV)	
			% of T_2 in N_e	0 and 10%	2

Some collisional processes induced by a fraction of 10% very energetic and hot electrons have been also considered at a temperature of T_{hot} = 10 keV. Other fractions of hot electrons have been tested with ATMED CR, observing a softer influence on parameters as mean charge than with the codes of Workshop NLTE-4, supposing an additive contribution of atomic processes. The collisional ionization rate from i energy level is calculated as follows:

$$I_C^{ic} = 4\pi a_0^2 Ryd^2 \zeta_{Lotz} c \left(\frac{8}{\pi m_e c^2} \right)^{1/2} \frac{N_e^{hot}}{(K_B T_e^{hot})^{3/2}} \frac{E_1(\beta_e^{hot} I_i)}{\beta_e^{hot} I_i} \quad (s^{-1}) \tag{1}$$

- $a_0 = 0.5291772083 \times 10^{-8}\ cm$: Bohr radius.
- $Ryd = -13.605698\ \ eV$: Hydrogen atom fundamental state energy.
- $\zeta_{Lotz} = 0.691$: Lozt approximation parameter.
- $c = 299792458 \times 10^2\ cm/s$: Speed of light.
- $m_e c^2 = mc = 0.510998902 \times 10^6\ \ eV$: Electron mass at rest.
- $N_e^{hot} = 0.1 * N_e$: Electronic density of hot electrons as a fraction of total density N_e .
- $T_e^{hot}\ eV$: Electronic temperature of hot electrons (10000 eV in these plasma cases) and $\beta_e^{hot} = 1 / K_B T_e^{hot}$ inverse of hot electrons temperature.
- $E_1(u) = \int_1^{\infty} dx \frac{e^{-ux}}{x}$: First exponential integral.
- $I_i = -\epsilon_i\ \ eV$: Ionization potential of energy level i.

The formula can be rewritten in an adequate form to implement it inside FORTRAN code as:

$$I_C^{ic} = 4.36\times10^{-6}\zeta_{Lotz}\frac{N_e^{hot}}{(K_B T_e^{hot})^{1/2} I_i} E_1(\beta_e^{hot} I_i) \quad (s^{-1}) \tag{2}$$

The rate of three body recombination to the energy level i, is calculated assuming LTE through detailed balance with collisional ionization:

$$R_C^{ci} = I_C^{ic}\exp\left[-\beta_e^{hot}\left(\in_i - \mu_e\right)\right] \quad (s^{-1}) \tag{3}$$

Although the relation has been deduced from the hypothesis of equilibrium, this only depends on atomic magnitudes and on the temperature. For that reason, the equation will be valid in every situation always and when the free electron distribution is a maxwellian function. The collisional excitation rate from i energy level to j one is calculated as follows:

$$\tau_{ij}^C = 16Ryd^2 a_0^2 c\left(\frac{2\pi^3}{3m_e c^2}\right)^{1/2}\frac{f_{ij}}{D_j^0}\frac{N_e^{hot}}{(K_B T_e^{hot})^{3/2}}\frac{\exp(-\beta_e^{hot}\in_{ij})}{\beta_e^{hot}\in_{ij}}G(\beta_e^{hot}\in_{ij}) \quad (s^{-1}) \tag{4}$$

- $\in_{ij} = \in_j - \in_i \quad eV$: Excitation energy.
- f_{ij} : Bound-bound absorption oscillator strength from i energy level to j one.
- $G(u) = A + (Bu - Cu^2 + D)e^u E_1(u) + Cu$: Gaunt factor.
  - $\left\{\begin{matrix} A = 0.15 & si & n_j \neq n_i \\ A = 0.60 & si & n_j = n_i \end{matrix}\right\}$: Parameter A.
  - $B = C = 0$: Parameters B and C.
  - $D = 0.28$: Parameter D.

The formula can be rewritten in an adequate form to implement it inside FORTRAN code as:

$$\tau_{ij}^C = 1.58\times10^{-5}\frac{f_{ij}}{\in_{ij}(K_B T_e^{hot})^{1/2}}\frac{N_e^{hot}}{D_j^0}\left[A\exp(-\beta_e^{hot}\in_{ij}) + 0.28E_1(\beta_e^{hot}\in_{ij})\right] \quad (s^{-1}) \tag{5}$$

The rate of collisional de-excitation from level j to level i, is calculated assuming LTE through detailed balance with collisional excitation:

$$\tau_{ji}^C = \tau_{ij}^C\exp\left[\beta_e^{hot}\left(\in_j - \in_i\right)\right] \quad (s^{-1}) \tag{6}$$

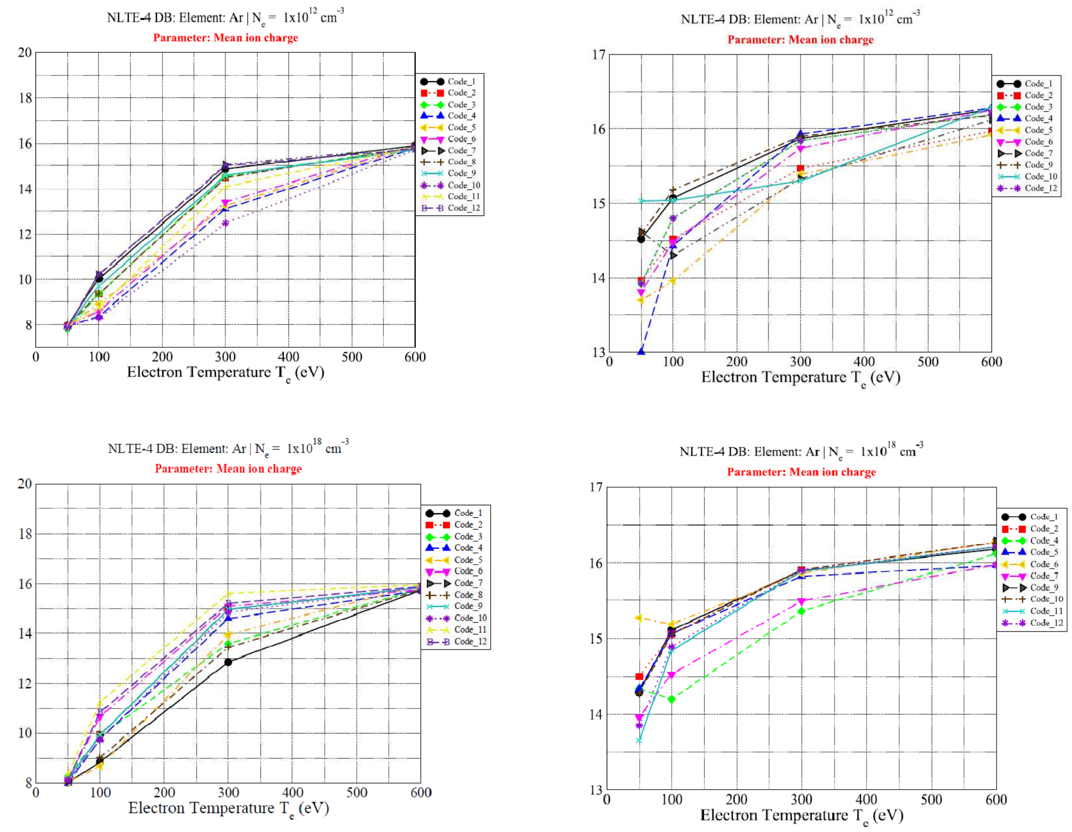

Figure 2.a. Argon plasma properties with participant codes of NLTE-4 Workshop, without (left) or with (right) hot electrons

Table 2.a: Argon plasma properties without hot electrons of ATMED CR for comparison with codes of NLTE-4 Workshop

0% Hot e- & N_e (cm^{-3}) = 10^{12}	ρ (g/cm^3)	Z_{bar} ATMED	Z_{bar} NLTE-4	η_e ATMED CR	K_R (cm^2/g)	K_P (cm^2/g)	RPL (1e-7 $J/cm^3/s$)
T_e = 100 eV	8.300E-12	7.999E+00	7.5÷11	-2.9428E+01	1.174E+01	1.420E+04	2.422328E+04
T_e = 300 eV	8.300E-12	8.017E+00	12÷15	-3.1074E+01	1.024E+02	4.465E+03	1.170868E+05
0% Hot e- & N_e (cm^{-3}) = 10^{18}	**ρ (g/cm^3)**	**Z_{bar} ATMED**	**Z_{bar} NLTE-4**	**η_e ATMED CR**	**K_R (cm^2/g)**	**K_P (cm^2/g)**	**RPL (1e-7 $J/cm^3/s$)**
T_e = 50 eV	8.300E-06	8.001E+00	8÷9	-1.4573E+01	1.175E+02	8.527E+03	5.394289E+14
T_e = 100 eV	8.900E-06	9.616E+00	9÷11	-1.5359E+01	1.495E+02	9.906E+03	2.107586E+15
T_e = 300 eV	5.700E-06	1.183E+01	11÷15	-1.7245E+01	2.988E+02	2.507E+03	8.107686E+15
T_e = 600 eV	5.500E-06	1.294E+01	15÷16	-1.8231E+01	2.281E+02	8.831E+02	1.977565E+16
0% Hot e- & N_e (cm^{-3}) = 10^{23}	**ρ (g/cm^3)**	**Z_{bar} ATMED**	**Z_{bar} NLTE-4**	**η_e ATMED CR**	**K_R (cm^2/g)**	**K_P (cm^2/g)**	**RPL (1e-7 $J/cm^3/s$)**
T_e = 100 eV	1.130E+00	5.907E+00	8÷10	-4.0884E+00	6.302E+03	1.133E+04	2.566309E+27
T_e = 300 eV	4.600E-01	1.458E+01	14÷16	-5.7365E+00	7.302E+01	5.008E+02	8.305196E+25
T_e = 600 eV	4.250E-01	1.577E+01	15÷16	-6.7773E+00	6.215E+00	3.186E+02	3.273017E+25

Table 2.b: Argon plasma properties of ATMED CR for other test cases with 50% of hot electrons

50% Hot e- & N_e (cm^{-3})	ρ (g/cm^3)	Z_{bar} ATMED	η_e ATMED CR	K_R (cm^2/g)	K_P (cm^2/g)	N_e (cm^{-3})
T_e = 100 eV	7.000E-06	1.022E+01	-1.5538E+01	1.215E+02	8.676E+03	1.0E+18
T_e = 100 eV	8.200E-01	8.161E+00	-4.0858E+00	4.475E+03	8.810E+03	1.0E+23
T_e = 300 eV	4.400E-01	1.530E+01	-5.7325E+00	3.153E+01	2.515E+02	1.0E+23

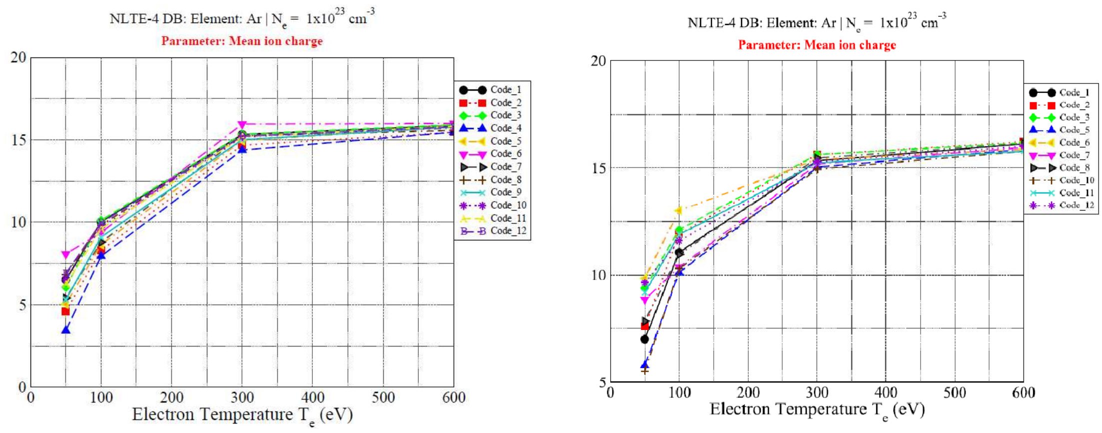

Figure 2.b. Argon plasma properties with participant codes of NLTE-4 Workshop, without (left) or with (right) hot electrons

Table 2.c: Argon plasma properties with hot electrons of ATMED CR for comparison with codes of NLTE-4 Workshop

10% Hot e- & N_e (cm^{-3}) = 10^{12}	ρ (g/cm^3)	Z_{bar} ATMED	Z_{bar} NLTE-4	η_e ATMED CR	K_R (cm^2/g)	K_P (cm^2/g)
T_e = 50 eV	9.000E-12	8.019E+00	13÷15	-2.8305E+01	1.624E+00	8.456E+03
T_e = 100 eV	8.500E-12	8.004E+00	14÷15	-2.9404E+01	1.006E+01	1.418E+04
T_e = 300 eV	8.300E-12	8.019E+00	15÷16	-3.1074E+01	1.012E+02	4.465E+03
10% Hot e- & N_e (cm^{-3}) = 10^{18}	**ρ (g/cm^3)**	**Z_{bar} ATMED**	**Z_{bar} NLTE-4**	**η_e ATMED CR**	**K_R (cm^2/g)**	**K_P (cm^2/g)**
T_e = 50 eV	8.200E-06	8.207E+00	13.5÷15	-1.4559E+01	6.618E+01	8.133E+03
T_e = 100 eV	7.000E-06	9.624E+00	14÷15	-1.5598E+01	1.420E+02	9.889E+03
T_e = 300 eV	5.700E-06	1.189E+01	15÷16	-1.7240E+01	2.960E+02	2.470E+03
T_e = 600 eV	5.500E-06	1.298E+01	16÷17	-1.8228E+01	2.269E+02	8.780E+02
10% Hot e- & N_e (cm^{-3}) = 10^{23}	**ρ (g/cm^3)**	**Z_{bar} ATMED**	**Z_{bar} NLTE-4**	**η_e ATMED CR**	**K_R (cm^2/g)**	**K_P (cm^2/g)**
T_e = 100 eV	1.700E+00	4.020E+00	10÷13	-4.0647E+00	7.890E+03	1.317E+04
T_e = 300 eV	4.600E-01	1.449E+01	15	-5.7423E+00	7.662E+01	5.223E+02
T_e = 600 eV	4.250E-01	1.573E+01	15÷16	-6.7799E+00	7.823E+00	3.151E+02

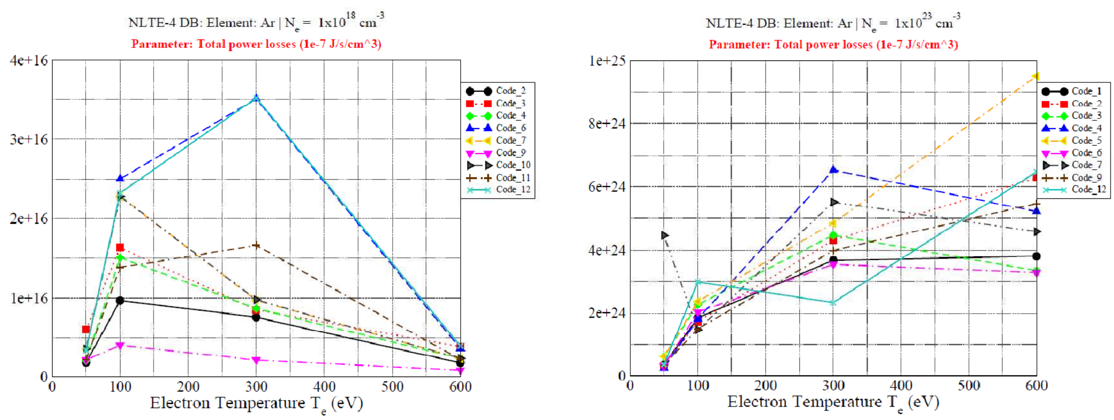

Figure 2.c. Argon plasma RPL with participant codes of NLTE-4 Workshop, without hot electrons

2.3 Tin Plasmas

The following problems have been established for the steady-state tin atoms, see Table 3, Figure 3:

Element	Case ID	Total # of Points	Parameter	Grid	# of Points
EUV lithography; includes optically thick case; spectrum emission; exp. data available					
Tin	Sn	50	T_e	20, 25, 30, 35, 40	5
			N_e	10^{18}, 5×10^{18}, 10^{19}, 5×10^{19}, 10^{21}	5
			Opacity	**r** = **0** and **0.1** mm; **L** = 5**r**	2
			Spectrum	**100−180** Å, $\Delta\lambda$ = **0.02** Å	4001
				Spectrum for N_e = 5×10^{18} only	

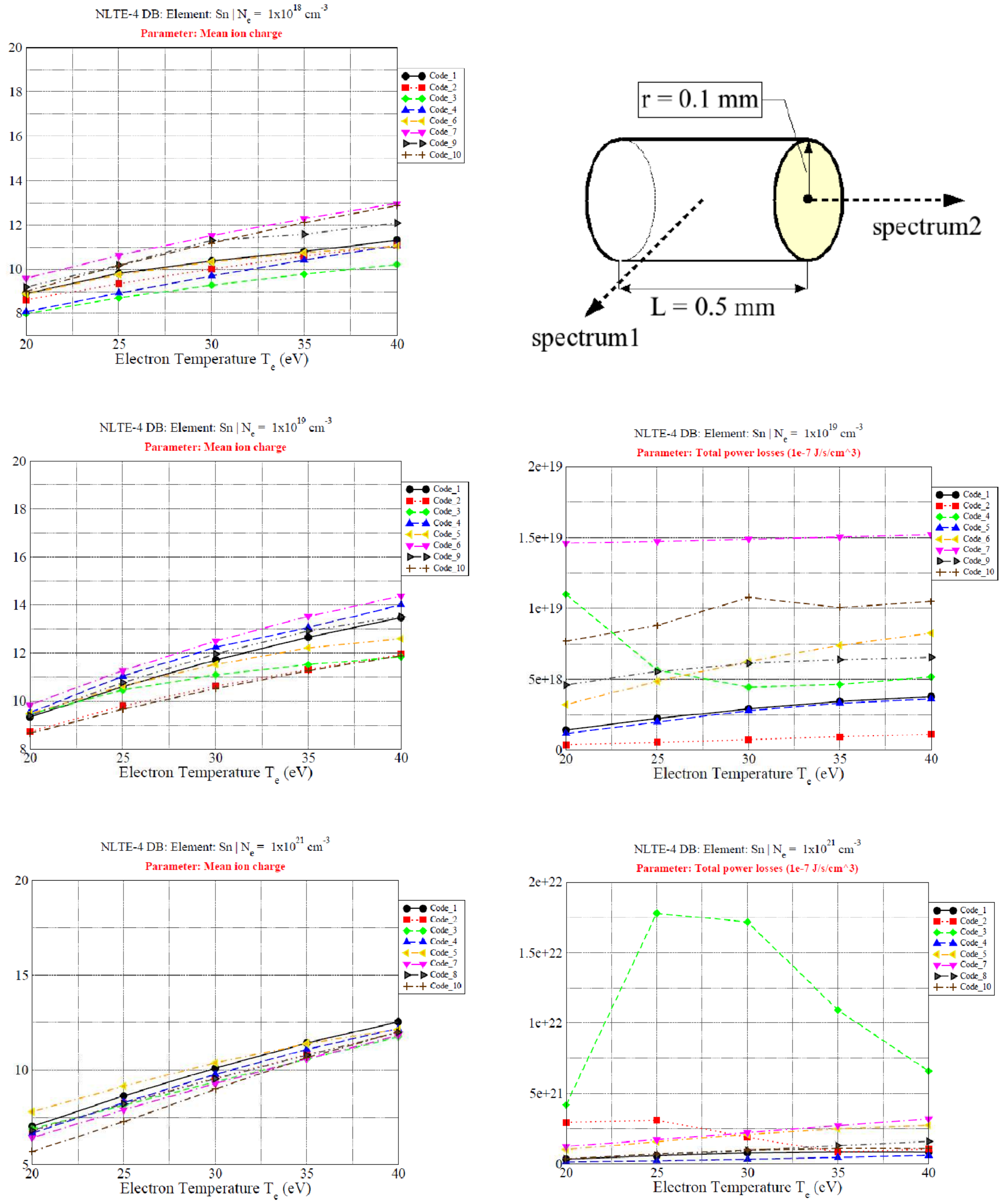

Figure 3.a. Tin plasma properties with participant codes of NLTE-4 Workshop. Thick cases by a uniform cylinder of radius 0.1 mm

Table 3.a: Tin optically thin plasma properties of ATMED CR for comparison with codes of NLTE-4 Workshop

r = 0 mm & N_e (cm^{-3}) = 10^{18}	ρ (g/cm^3)	Z_{bar} ATMED	Zbar NLTE-4	η_e ATMED CR	K_R (cm^2/g)	K_P (cm^2/g)	RPL (1e-7 $J/cm^3/s$)
T_e = 25 eV	2.200E-05	9.048E+00	8.5÷10.5	-1.3524E+01	4.438E+03	7.422E+04	8.211182E+15
T_e = 30 eV	2.000E-05	1.015E+01	9.25÷11.5	-1.3778E+01	5.562E+03	5.958E+04	1.406701E+16
T_e = 40 eV	1.800E-05	1.137E+01	10.2÷13	-1.4201E+01	6.183E+03	4.021E+04	3.135937E+16
r = 0 mm & N_e (cm^{-3}) = 10^{19}	**ρ (g/cm^3)**	**Z_{bar} ATMED**	**Zbar NLTE-4**	**η_e ATMED CR**	**K_R (cm^2/g)**	**K_P (cm^2/g)**	**RPL (1e-7 $J/cm^3/s$)**
T_e = 20 eV	2.200E-04	8.990E+00	8.6÷9.8	-1.0893E+01	7.889E+03	7.161E+04	3.570959E+17
T_e = 30 eV	1.690E-04	1.172E+01	10.5÷12.5	-1.1500E+01	7.240E+03	4.791E+04	9.072992E+17
T_e = 40 eV	1.610E-04	1.318E+01	11.8÷14.4	-1.1863E+01	2.974E+03	3.085E+04	2.034111E+18
r = 0 mm & N_e (cm^{-3}) = $5x10^{19}$	**ρ (g/cm^3)**	**Z_{bar} ATMED**	**Zbar NLTE-4**	**η_e ATMED CR**	**K_R (cm^2/g)**	**K_P (cm^2/g)**	**RPL (1e-7 $J/cm^3/s$)**
T_e = 20 eV	1.128E-03	8.744E+00	8.6÷9.8	-9.2865E+00	1.346E+04	7.371E+04	1.155404E+19
T_e = 30 eV	8.320E-04	1.186E+01	10.8÷12.4	-9.8943E+00	8.778E+03	4.670E+04	1.502173E+19
T_e = 40 eV	7.060E-04	1.398E+01	12.2÷14.6	-1.0325E+01	3.323E+03	2.689E+04	2.350469E+19
r = 0 mm & N_e (cm^{-3}) = 10^{21}	**ρ (g/cm^3)**	**Z_{bar} ATMED**	**Zbar NLTE-4**	**η_e ATMED CR**	**K_R (cm^2/g)**	**K_P (cm^2/g)**	**RPL (1e-7 $J/cm^3/s$)**
T_e = 20 eV	3.000E-02	6.884E+00	6.4÷8	-6.2443E+00	2.987E+04	9.324E+04	7.896211E+23
T_e = 30 eV	2.100E-02	9.680E+00	9÷10.5	-6.8686E+00	2.404E+04	6.128E+04	3.156075E+22
T_e = 40 eV	1.700E-02	1.216E+01	11.75÷12.5	-7.2837E+00	1.006E+04	3.448E+04	4.486346E+22

Table 3.b: Tin optically thick plasma properties of ATMED CR for comparison with codes of NLTE-4 Workshop

r = 0.1 mm & N_e (cm^{-3}) = 10^{18}	ρ (g/cm^3)	Z_{bar} ATMED	Zbar NLTE-4	η_e ATMED CR	K_R (cm^2/g)	K_P (cm^2/g)	RPL (1e-7 $J/cm^3/s$)
T_e = 25 eV	2.200E-05	9.208E+00	8.5÷10.5	-1.3507E+01	4.542E+03	7.257E+04	8.051135E+15
T_e = 30 eV	2.000E-05	1.026E+01	9.25÷11.5	-1.3767E+01	5.540E+03	5.862E+04	1.337473E+16
T_e = 40 eV	1.800E-05	1.145E+01	10.2÷13	-1.4195E+01	6.001E+03	3.979E+04	2.970821E+16
r = 0.1 mm & N_e (cm^{-3}) = 10^{19}	**ρ (g/cm^3)**	**Z_{bar} ATMED**	**Zbar NLTE-4**	**η_e ATMED CR**	**K_R (cm^2/g)**	**K_P (cm^2/g)**	**RPL (1e-7 $J/cm^3/s$)**
T_e = 20 eV	2.200E-04	9.512E+00	8.6÷9.8	-1.0837E+01	8.693E+03	6.667E+04	3.859802E+17
T_e = 30 eV	1.690E-04	1.210E+01	10.5÷12.5	-1.1468E+01	5.492E+03	4.548E+04	9.198930E+17
T_e = 40 eV	1.500E-04	1.349E+01	11.8÷14.4	-1.1911E+01	2.646E+03	2.945E+04	1.881815E+18
r = 0.1 mm & N_e (cm^{-3}) = $5x10^{19}$	**ρ (g/cm^3)**	**Z_{bar} ATMED**	**Zbar NLTE-4**	**η_e ATMED CR**	**K_R (cm^2/g)**	**K_P (cm^2/g)**	**RPL (1e-7 $J/cm^3/s$)**
T_e = 20 eV	1.090E-03	9.045E+00	8.6÷9.8	-9.2869E+00	1.400E+04	7.075E+04	1.056407E+19
T_e = 30 eV	8.040E-04	1.228E+01	10.8÷12.4	-9.8939E+00	6.712E+03	4.408E+04	1.384552E+19
T_e = 40 eV	6.680E-04	1.476E+01	12.2÷14.8	-1.0327E+01	2.569E+03	2.378E+04	2.100325E+19
r = 0.1 mm & N_e (cm^{-3}) = 10^{21}	**ρ (g/cm^3)**	**Z_{bar} ATMED**	**Zbar NLTE-4**	**η_e ATMED CR**	**K_R (cm^2/g)**	**K_P (cm^2/g)**	**RPL (1e-7 $J/cm^3/s$)**
T_e = 20 eV	3.000E-02	6.898E+00	6.4÷8	-6.2422E+00	2.986E+04	9.305E+04	2.814807E+22
T_e = 30 eV	2.100E-02	9.714E+00	9÷10.5	-6.8650E+00	2.388E+04	6.097E+04	1.494380E+22
T_e = 40 eV	1.700E-02	1.223E+01	11.75÷12.5	-7.2775E+00	9.765E+03	3.410E+04	1.104052E+22

2.4 Xenon Plasmas

The following problems have been established for the steady-state cases of xenon atoms on a grid of electron temperatures and electron densities, see Table 4 and Figure 4:

Element	Case ID	Total # of Points	Parameter	Grid	# of Points
Radiation power loss case					
Xenon	Xe	27	T_e	10, 20, 50, 100, 200, 500, 1000, 2000, 5000	9
			N_e	10^{14}, 10^{18}, 10^{22}	3

For the densities 1E+18 and 1E+22 cm^{-3}, at high temperatures the autoionization rate would be used with an upper limit [2,21]:

$$A_{ji}^{kc} = C_{auto} \tanh\left[\frac{3\pi}{2\hbar} \left(\frac{\epsilon_j - \epsilon_i}{Z_{bar}} \right)^2 \frac{f_{ij}}{D_j^0} \left. \frac{df_k}{d\epsilon} \right|_{\epsilon=-\epsilon_k} \frac{g_A}{C_{auto}} \right] \qquad (7)$$

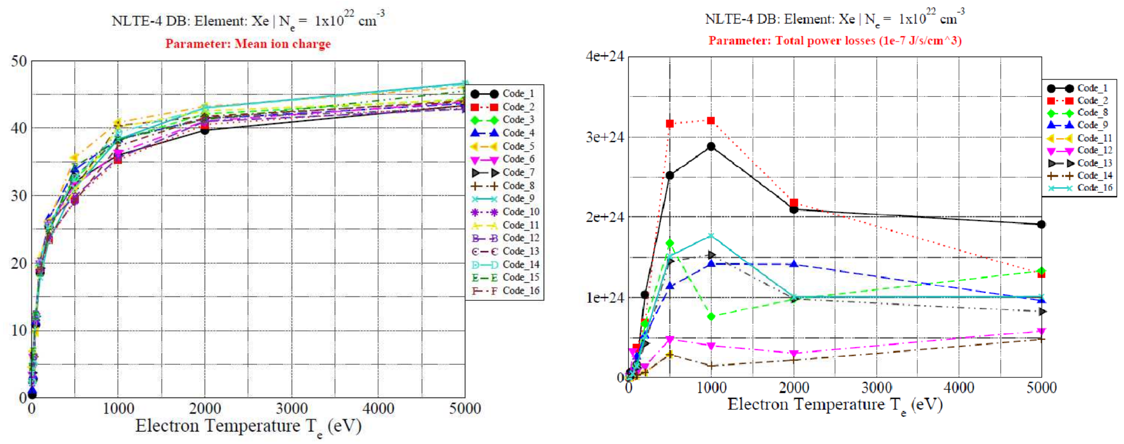

Figure 4.a. Xenon plasma properties computed with participant codes of NLTE-4 Workshop

Table 4.a: Xenon plasma properties of ATMED CR for comparison with codes of NLTE-4 Workshop

N_e (cm^{-3}) = 10^{22}	ρ (g/cm^3)	Z_{bar} ATMED	Z_{bar} NLTE-4	η_e ATMED CR	K_R (cm^2/g)	K_P (cm^2/g)	RPL (1e-7 J/cm^3/s)
T_e = 20 eV	9.000E-01	2.548E+00	2÷7	-3.9315E+00	9.366E+04	1.333E+05	2.533781E+26
T_e = 50 eV	2.300E-01	9.973E+00	9.8÷13	-5.3108E+00	1.628E+04	3.662E+04	4.102854E+25
T_e = 100 eV	1.200E-01	1.850E+01	18÷21	-6.3846E+00	2.651E+03	6.972E+03	6.319852E+24
T_e = 200 eV	9.000E-02	2.530E+01	23÷27	-7.3990E+00	4.610E+02	3.514E+03	3.734867E+24
T_e = 500 eV	7.500E-02	2.999E+01	29÷36	-8.7859E+00	3.927E+02	1.737E+03	4.593139E+23
T_e = 1000 eV	7.000E-02	3.357E+01	33÷41	-9.7820E+00	2.867E+02	7.925E+02	4.349219E+23
T_e = 2000 eV	7.500E-02	3.699E+01	40÷43	-1.0656E+01	8.463E+01	3.754E+02	7.626696E+23
T_e = 5000 eV	6.000E-02	3.960E+01	43÷47	-1.2185E+01	1.388E+01	7.945E+01	9.240009E+23

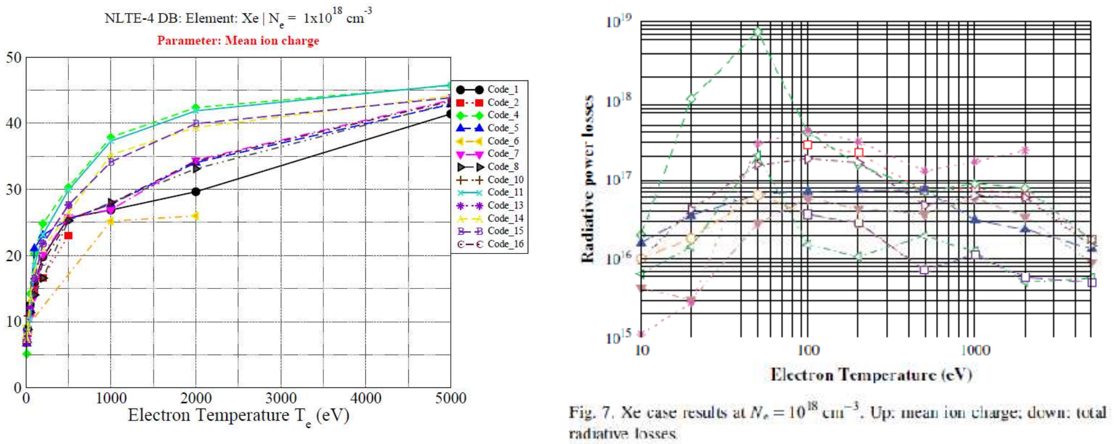

Figure 4.b. Xenon plasma properties computed with participant codes of NLTE-4 Workshop

Table 4.b: Xenon plasma properties of ATMED CR for comparison with codes of NLTE-4 Workshop

N_e (cm^{-3}) = 10^{18}	ρ (g/cm^3)	Z_{bar} ATMED	Z_{bar} NLTE-4	η_e ATMED CR	K_R (cm^2/g)	K_P (cm^2/g)	RPL (1e-7 J/cm^3/s)
T_e = 10 eV	3.300E-05	7.142E+00	5÷8	-1.2082E+01	1.048E+03	1.561E+04	1.483998E+16
T_e = 20 eV	2.500E-05	8.761E+00	7.8÷11	-1.3195E+01	9.298E+02	5.679E+04	5.267371E+15
T_e = 50 eV	1.800E-05	1.213E+01	10÷14	-1.4572E+01	4.764E+03	3.663E+04	2.678358E+16
T_e = 100 eV	1.500E-05	1.550E+01	15÷25	-1.5549E+01	2.062E+03	1.172E+04	1.154369E+17
T_e = 200 eV	1.300E-05	1.804E+01	17÷25	-1.6580E+01	1.451E+03	5.882E+03	2.733019E+17
T_e = 500 eV	1.000E-05	2.349E+01	17÷30	-1.7953E+01	3.870E+02	2.306E+03	4.788253E+17
T_e = 1000 eV	9.000E-06	2.583E+01	25÷37	-1.9003E+01	2.600E+02	1.011E+03	3.433794E+17
T_e = 2000 eV	8.000E-06	2.808E+01	26÷42	-2.0077E+01	9.238E+01	4.289E+02	2.503671E+17

With ATMED CR, optically coronal thin plasmas have been modeled without external radiation field and considering the Albritton's formula without upper limit for the atomic processes autoionization and dielectronic capture. The autoionization rate is calculated through the approximated expression:

$$A_{ji}^{kc} = \frac{3\pi}{2\hbar}\left(\frac{\in_j - \in_i}{Z_{bar}}\right)^2 \frac{f_{ij}}{D_j^0} \left.\frac{df_k}{d\in}\right|_{\in=-\in_k} g_A \tag{8}$$

Without the upper limit the splitting is of maximum importance for the bound-free oscillator strength of an electron that being bound to the nucleus, experiments a transition to the continuum. Different properties are computed if it corresponds to one or the other one between the next formulas:

- Bound-free oscillator strength formula belonging to the atomic NRSHM depending on the principal and orbital quantum numbers [2]:

$$\left.\frac{df_k}{d\in}\right|_{\in=-\in_k} = f_{nl,\in_c l'} = \frac{l+l'+1}{3(2l+1)} r_{nl,\in l'}^2 \tag{9}$$

- Bound-free oscillator strength formula depending on the principal quantum number [8]:

$$\left.\frac{df_k}{d\in}\right|_{\in=-\in_k} \Rightarrow \frac{f_{n,\in_c}}{-\in_k\,(eV)} = \frac{12\,\dfrac{Q_k^4}{A}\,\dfrac{1}{n^5(k)}}{-\in_k\,(eV)} \tag{10}$$

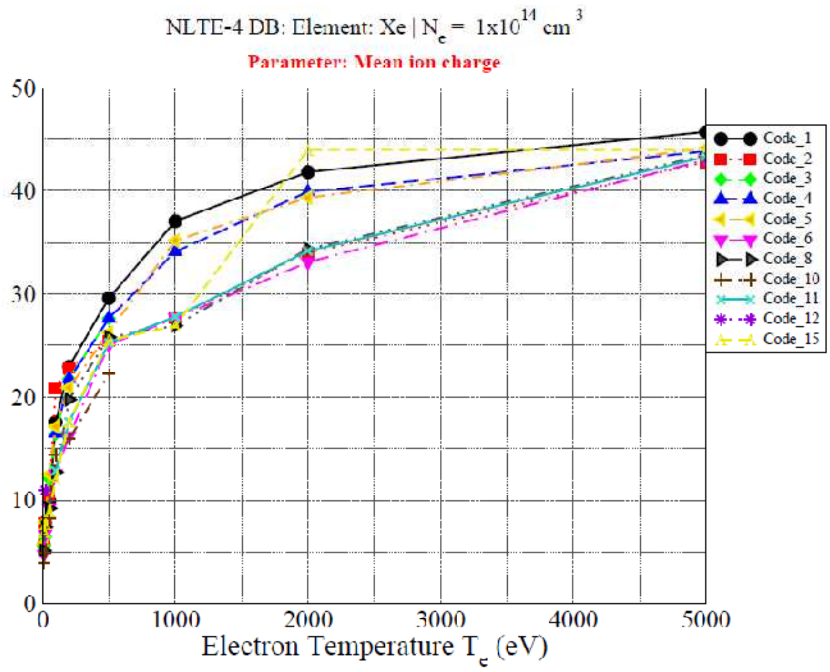

Figure 4.c. Xenon plasma properties computed with participant codes of NLTE-4 Workshop in coronal regime

Table 4.c: Xenon plasma properties of ATMED CR and splitting of bound-free oscillator strength (nl) or (n)

nl-splitting & N_e (cm^{-3}) = 10^{14}	**ρ (g/cm^3)**	**Z_{bar} ATMED**	**Z_{bar} NLTE-4**	**η_e ATMED CR**	**K_R (cm^2/g)**	**K_P (cm^2/g)**	**RPL (1e-7 J/cm^3/s)**
T_e = 10 eV	2.730E-09	8.035E+00	4÷10	-2.1364E+01	1.363E+01	8.131E+03	8.514073E+09
T_e = 50 eV	2.150E-09	1.016E+01	10÷18	-2.3782E+01	5.165E+02	4.797E+04	1.637669E+10
T_e = 100 eV	1.915E-09	1.145E+01	10÷18	-2.4818E+01	1.673E+03	1.823E+04	3.123356E+10
T_e = 200 eV	1.900E-09	1.384E+01	16÷24	-2.5676E+01	2.977E+03	7.438E+03	1.420837E+11
T_e = 500 eV	1.200E-09	1.818E+01	22÷30	-2.7237E+01	4.581E+02	2.784E+03	5.970642E+10
T_e = 1000 eV	8.500E-10	2.571E+01	25÷37	-2.8275E+01	1.271E+02	1.017E+03	1.321816E+10
T_e = 2000 eV	7.400E-10	2.952E+01	34÷44	-2.9316E+01	9.234E+01	4.237E+02	8.727946E+09
n-splitting & N_e (cm^{-3}) = 10^{14}	**ρ (g/cm^3)**	**Z_{bar} ATMED**	**Z_{bar} NLTE-4**	**η_e ATMED CR**	**K_R (cm^2/g)**	**K_P (cm^2/g)**	**RPL (1e-7 J/cm^3/s)**
T_e = 200 eV	8.400E-10	2.600E+01	16÷24	-2.5862E+01	4.607E+00	3.582E+03	1.517194E+11
T_e = 500 eV	8.400E-10	2.605E+01	22÷30	-2.7234E+01	2.323E+01	2.186E+03	2.739240E+11
T_e = 1000 eV	8.360E-10	2.622E+01	25÷37	-2.8272E+01	1.094E+02	1.007E+03	2.453132E+11
T_e = 2000 eV	5.000E-10	4.397E+01	34÷44	-2.9309E+01	2.513E+00	3.110E+02	3.228842E+12

2.5 Gold Plasmas

The following problems have been established for the steady-state cases of gold atoms on a grid of electron temperatures and electron densities:

Element	Case ID	Total # of Points	Parameter	Grid	# of Points
Comparison with experimental data; Planckian radiation field					
Gold	Au	48	T_e	400, 870, 1400, 2000, 2500, 5000	6
			N_e	3×10^{20}, 10^{21}, 3×10^{21}, 10^{22}	4
			T_{rad}	0, 175	2
			Spectrum	**2.8−4.4** Å, Δλ = **0.001** Å	1601

If the upper limit used is $C_{auto} = 10^{14}\ s^{-1}$ at high temperatures the values in Table 5 are obtained. This figure has been established according to Ref. [10] for matching plasma properties of a specific experiment of iron with values of temperatures at around 150 eV. Greater values more centered in the range of the rest of codes for higher temperatures can be computed with other formulas with upper limit of the order of magnitude $10^{17}\ s^{-1}$, see References [22,23] . So this limit must be adjusted according to real experimental values for calculations.

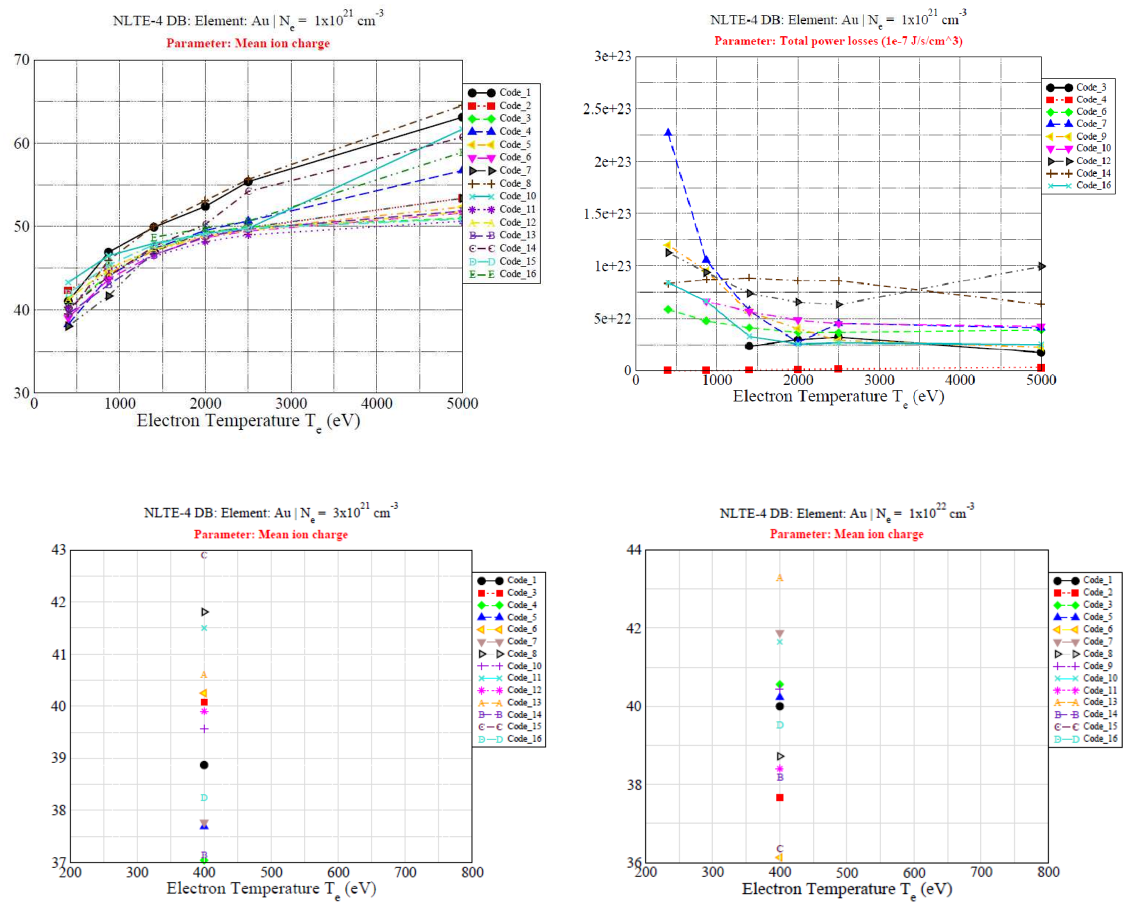

Figure 5.a. Gold plasma properties at radiation temperature T_{rad} = 175 eV computed with participant codes of NLTE-4 Workshop

Table 5.a: Gold plasma properties of ATMED CR for comparison with codes of NLTE-4 Workshop

T_{rad} = 175 eV & N_e (cm^{-3}) = $3x10^{20}$	ρ (g/cm^3)	Z_{bar} ATMED	Z_{bar} NLTE-4	η_e ATMED CR	RPL (1e-7 $J/cm^3/s$)
T_e = 400 eV	2.389E-03	4.108E+01	40÷45	-1.1989E+01	1.258219E+22
T_e = 870 eV	2.298E-03	4.275E+01	42÷47	-1.3154E+01	1.359198E+22
T_e = 1400 eV	2.207E-03	4.446E+01	46÷50	-1.3868E+01	1.527139E+22
T_e = 2000 eV	2.136E-03	4.594E+01	49÷53	-1.4403E+01	1.106929E+22
T_e = 2500 eV	2.086E-03	4.704E+01	49÷55	-1.4738E+01	4.634427E+22
T_e = 5000 eV	1.991E-03	4.929E+01	49÷65	-1.5778E+01	7.409020E+21
T_{rad} = 175 eV & N_e (cm^{-3}) = 10^{21}	ρ (g/cm^3)	Z_{bar} ATMED	Z_{bar} NLTE-4	η_e ATMED CR	RPL (1e-7 $J/cm^3/s$)
T_e = 400 eV	8.253E-03	3.964E+01	38÷43	-1.0785E+01	1.421529E+18
T_e = 870 eV	7.773E-03	4.209E+01	43÷47	-1.1950E+01	1.138915E+18
T_e = 1400 eV	7.346E-03	4.453E+01	46÷50	-1.2664E+01	8.685890E+17
T_e = 2000 eV	7.059E-03	4.633E+01	49÷53	-1.3199E+01	5.918562E+22
T_e = 2500 eV	6.888E-03	4.749E+01	49÷55	-1.3534E+01	1.133327E+24
T_e = 5000 eV	6.586E-03	4.966E+01	49÷65	-1.4574E+01	3.965581E+17
T_{rad} = 175 eV & N_e (cm^{-3}) = $3x10^{21}$	ρ (g/cm^3)	Z_{bar} ATMED	Z_{bar} NLTE-4	η_e ATMED CR	RPL (1e-7 $J/cm^3/s$)
T_e = 400 eV	2.530E-02	3.878E+01	37÷43	-9.6865E+00	4.767750E+18
T_e = 870 eV	2.315E-02	4.239E+01	44÷47	-1.0852E+01	2.266840E+23
T_e = 1400 eV	2.185E-02	4.492E+01	46÷50	-1.1565E+01	2.536505E+23
T_e = 2000 eV	2.092E-02	4.691E+01	49÷53	-1.2100E+01	3.648669E+25
T_e = 2500 eV	2.045E-02	4.798E+01	49÷55	-1.2435E+01	2.551228E+23
T_e = 5000 eV	1.962E-02	5.001E+01	49÷65	-1.3475E+01	1.616903E+25
T_{rad} = 175 eV & N_e (cm^{-3}) = 10^{22}	ρ (g/cm^3)	Z_{bar} ATMED	Z_{bar} NLTE-4	η_e ATMED CR	RPL (1e-7 $J/cm^3/s$)
T_e = 400 eV	8.485E-02	3.856E+01	36÷43	-8.4821E+00	1.007452E+24
T_e = 870 eV	7.554E-02	4.330E+01	44÷47	-9.6479E+00	4.356268E+25
T_e = 1400 eV	7.170E-02	4.561E+01	47÷50	-1.0362E+01	8.475453E+25
T_e = 2000 eV	6.875E-02	4.758E+01	49÷53	-1.0897E+01	3.242478E+26
T_e = 2500 eV	6.740E-02	4.853E+01	49÷55	-1.1231E+01	1.006861E+27
T_e = 5000 eV	6.467E-02	5.058E+01	49÷65	-1.2271E+01	3.848314E+18

The mean charge values calculated with ATMED CR are always more approximated to the ones of detailed models considering a very complete selection of configurations with respect to other selections with a more reduced number of configurations [21]. For these atomic processes ATMED CR considers all possible combinations between three energy orbitals which comply with the aforementioned restrictions on their binding energies through the formula (7). The detailed model of reference [21] has considered different types of doubly excited states, also called autoionizing states which can decay through the autoionization channel, obtaining several models denominated A, B, C and D. This way model A has the greatest number of configurations, typically, some thousands. The number of configurations in model C is around 90% of the ones included in model A, while in model D, the number is the half of that in model A.

It has been checked in the ranges of density (1E+20÷1E+21 cm^{-3}) and temperature (1000÷1500 eV) in which there is greater discrepancy between models, see Table 5 and Figure 5, that calculations of mean charge with ATMED CR, are more similar to the results of models A and C more complete in number of selected configurations and autoionizing states [2].

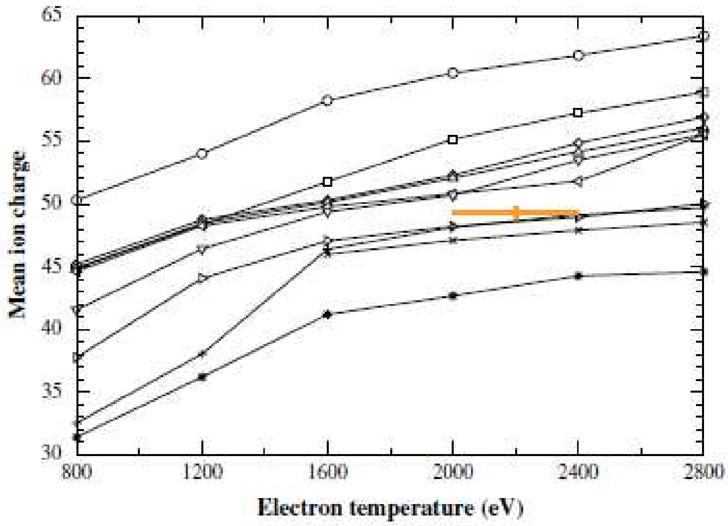

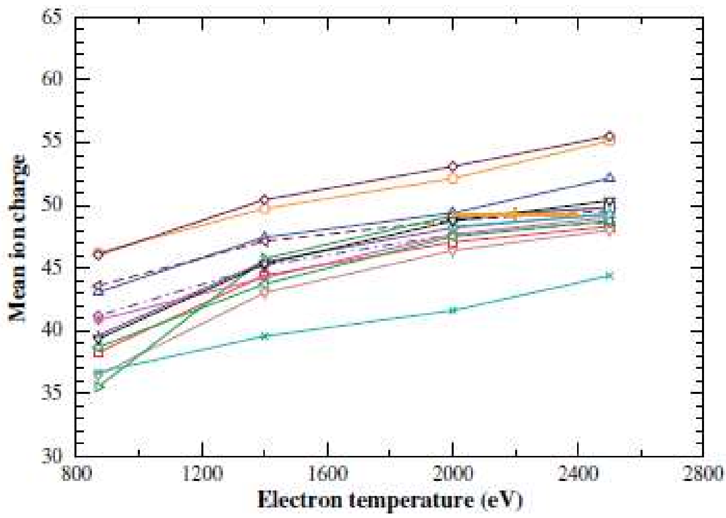

Figure 5.b. Mean ion charge for Au as a function of electronic temperature. NLTE-1 results at N_e = 1.0E+20 cm^{-3} (above); NLTE-4 results at N_e = 3.0E+20 cm^{-3} (below). The experimental value at T_e = 2200 eV, N_e = 6.0E+20 cm^{-3}, is Z_{bar} = 49.3 ± 0.5, in approximate agreement with the theory. Less data scatter of results obtained by codes at NLTE-4 with significant improvement in agreement in respect of NLTE-1.

Table 5.b: Gold plasma properties of ATMED CR for experimental case depending on bound-free oscillator strength splitting

BF nl-splitting & T_{rad} = 0 eV	N_e (cm^{-3})	ρ (g/cm^3)	Z_{bar} ATMED	η_e ATMED CR	RPL (1e-7 J/cm^3/s)
T_e = 2200 eV	6.0E+20	4.249E-03	4.619E+01	-1.3853E+01	4.852264E+22
BF n-splitting & T_{rad} = 0 eV	**N_e (cm^{-3})**	**ρ (g/cm^3)**	**Z_{bar} ATMED**	**η_e ATMED CR**	**RPL (1e-7 J/cm^3/s)**
T_e = 2200 eV	6.0E+20	4.200E-03	4.673E+01	-1.3853E+01	3.810040E+22

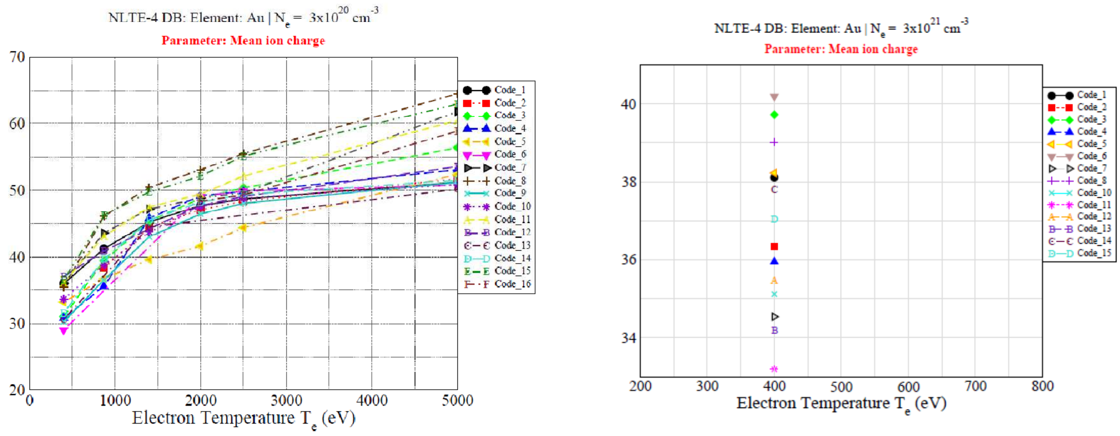

Figure 5.c. Gold plasma properties at radiation temperature T_{rad} = 0 eV computed with participant codes of NLTE-4 Workshop

Table 5.c: Gold plasma properties of ATMED CR for comparison with codes of NLTE-4 Workshop

T_{rad} = 0 eV & N_e (cm^{-3}) = 3x10^{20}	ρ (g/cm^3)	Z_{bar} ATMED	Z_{bar} NLTE-4	η_e ATMED CR	RPL (1e-7 J/cm^3/s)
T_e = 400 eV	3.427E-03	2.864E+01	28÷37	-1.1989E+01	5.986432E+18
T_e = 870 eV	2.850E-03	3.460E+01	35÷46	-1.3150E+01	7.725666E+21
T_e = 1400 eV	2.420E-03	4.079E+01	40÷50	-1.3862E+01	1.376220E+22
T_e = 2000 eV	2.186E-03	4.490E+01	42÷53	-1.4403E+01	1.520758E+22
T_e = 2500 eV	2.124E-03	4.623E+01	48÷57	-1.4737E+01	1.487068E+22
T_e = 5000 eV	2.025E-03	4.856E+01	50÷65	-1.5775E+01	2.801813E+22
T_{rad} = 0 eV & N_e (cm^{-3}) = 10^{21}	**ρ (g/cm^3)**	**Z_{bar} ATMED**	**Z_{bar} NLTE-4**	**η_e ATMED CR**	**RPL (1e-7 J/cm^3/s)**
T_e = 400 eV	1.034E-02	3.167E+01	31÷38	-1.0784E+01	2.921067E+22
T_e = 870 eV	8.692E-03	3.764E+01	37÷46	-1.1950E+01	6.527791E+22
T_e = 1400 eV	7.683E-03	4.257E+01	44÷50	-1.2664E+01	7.616660E+22
T_e = 2000 eV	7.135E-03	4.584E+01	48÷53	-1.3199E+01	7.767916E+22
T_e = 2500 eV	6.940E-03	4.717E+01	49÷56	-1.3533E+01	7.783407E+22
T_e = 5000 eV	6.610E-03	4.948E+01	50÷65	-1.4574E+01	6.891608E+22
T_{rad} = 0 eV & N_e (cm^{-3}) = 3x10^{21}	**ρ (g/cm^3)**	**Z_{bar} ATMED**	**Z_{bar} NLTE-4**	**η_e ATMED CR**	**RPL (1e-7 J/cm^3/s)**
T_e = 400 eV	2.882E-02	3.405E+01	33÷40	-9.6863E+00	1.800489E+23
T_e = 870 eV	2.405E-02	4.093E+01	40÷47	-1.0849E+01	2.401587E+23
T_e = 1400 eV	2.212E-02	4.436E+01	47÷50	-1.1566E+01	3.490663E+23
T_e = 2000 eV	2.102E-02	4.669E+01	47÷53	-1.2100E+01	2.559386E+23
T_e = 2500 eV	2.050E-02	4.786E+01	50÷57	-1.2436E+01	2.628926E+23
T_e = 5000 eV	1.964E-02	4.996E+01	51÷64	-1.3475E+01	2.118830E+23
T_{rad} = 0 eV & N_e (cm^{-3}) = 10^{22}	**ρ (g/cm^3)**	**Z_{bar} ATMED**	**Z_{bar} NLTE-4**	**η_e ATMED CR**	**RPL (1e-7 J/cm^3/s)**
T_e = 400 eV	9.013E-02	3.630E+01	34÷41	-8.4821E+00	9.711455E+23
T_e = 870 eV	7.686E-02	4.257E+01	42÷48	-9.6478E+00	1.341845E+24
T_e = 1400 eV	7.202E-02	4.541E+01	47÷50	-1.0362E+01	1.714135E+24
T_e = 2000 eV	6.888E-02	4.748E+01	49÷53	-1.0897E+01	1.116038E+24
T_e = 2500 eV	6.748E-02	4.847E+01	50÷57	-1.1231E+01	1.100801E+24
T_e = 5000 eV	6.469E-02	5.056E+01	52÷64	-1.2271E+01	9.142339E+23

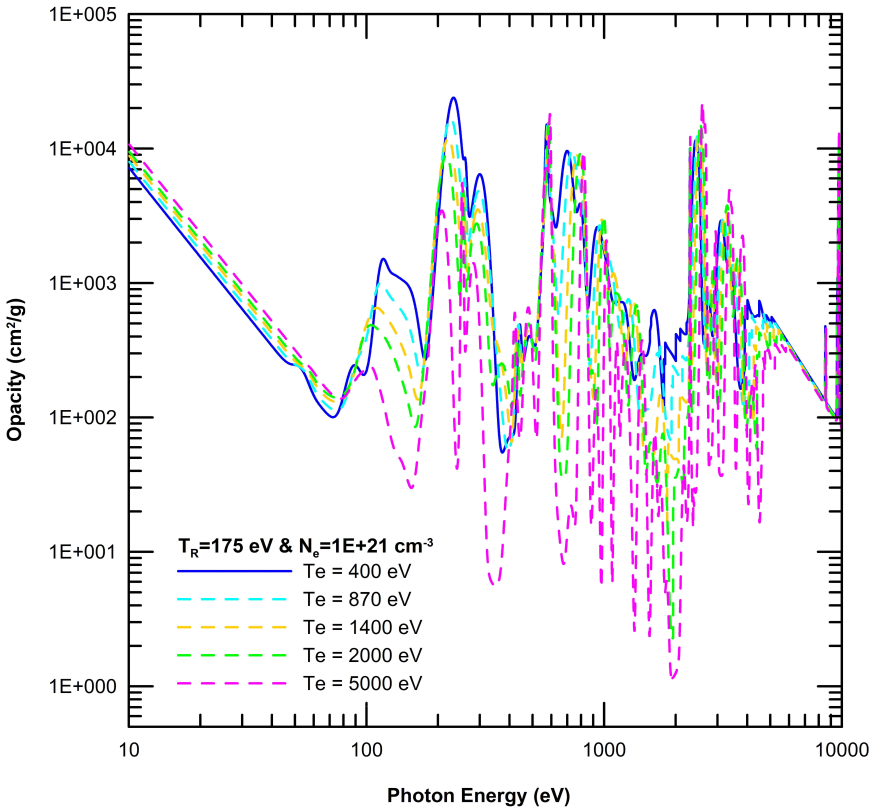

Figure 5.d. Gold plasma opacity computed with ATMED CR at radiation temperature T_{rad} = 175 eV at electronic temperatures in the range T_e = 400÷5000 eV and electronic density 1E+21 cm^{-3}

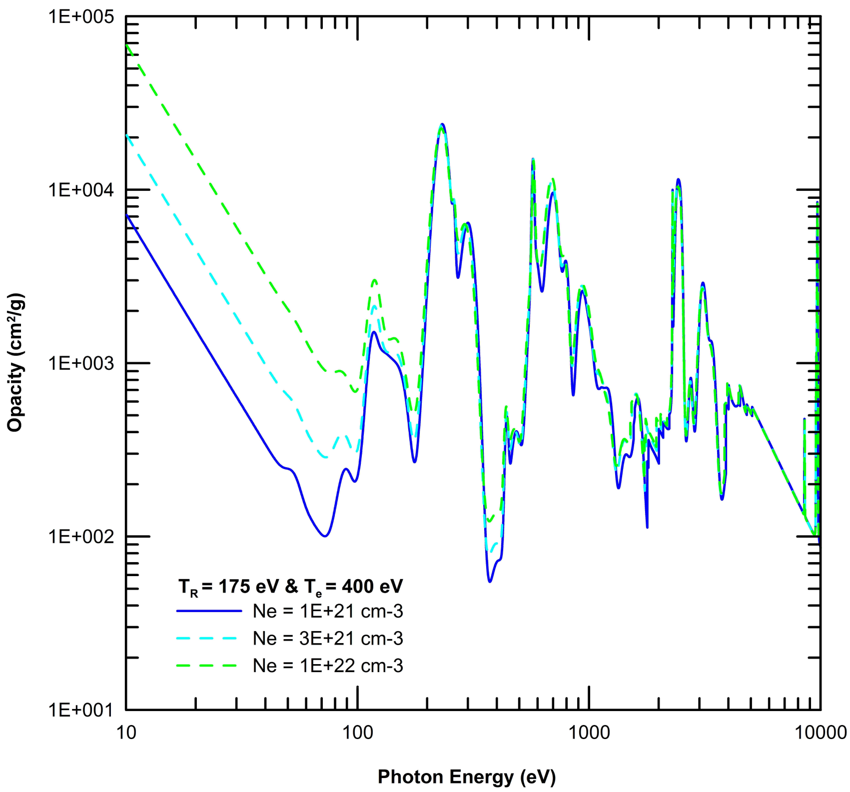

Figure 5.e. Gold plasma opacity computed with ATMED CR at radiation temperature T_{rad} = 175 eV at electronic temperature T_e = 400 eV and electronic densities in the range 1E+21÷1E+22 cm^{-3}

3. SUMMARY AND CONCLUSIONS

In this paper, there are modeled with ATMED CR steady-state plasmas proposed in the 4th Non-LTE Code Comparison Workshop held in December 2005. Cases for C, Ar, Fe, Sn, Xe and Au plasmas were selected for analyzing dense plasma physics, EUV lithography sources, cold plasmas, etc., see Figure 6.

Code	Contributors	Institution
ATOM3R [7]	Florido, Rubiano, Gil, Rodríguez, Mínguez, *Mancini*, Martel	ULPGC/DENIM, Spain
ATOMIC [8]	Fontes, Abdallah	LANL, USA
AVERROES [9]	Peyrusse, *Gilleron*	CELIA/CEA, France
CRETIN/CRETINL [10]	Scott	LLNL, USA
ECRSS [11]	*Salzmann*	Soreq NRC
FAC [12]	*Gu*	Centre for Space Research, USA
FLYCHK [13]	Chung, Lee	LLNL, USA
GONDOR [14]	Bowen	CEA, France
HULLAC v.9 [15]	Klapisch, Busquet	NRL/ARTEP, USA/France
JATOM [16]	Sasaki	JAEA, Japan
MOST/AVE [17]	Bauche-Arnoult, Bauche	Lab. Aimé-Cotton, France
NOHEL/NOHEL2E [2]	Decoster	CEA, France
NOMAD [18]	Ralchenko	NIST, USA
RADIOM [19]	Bowen	CEA, France
SCAALP [20]	Faussurier, Blancard	CEA, France
SCRAM [21]	Hansen	LLNL, USA
SCRIC [22]	de Gaufridy	CEA, France
SCROLL [23]	Klapish, Bar-Shalom, Oreg	NRL/NRCN/ARTEP, USA/Israel
THERMOS [24]	Novikov	Keldysh Institute. Russian Academy of Sciences
XSTAR [25]	*Kallman*	NASA Goddard Space Flight Centre, USA

Code	C	Ar	Fe	Sn	Xe	Au	TD-Ar
ATOM3R	x				x		
ATOMIC	x	x	x	x	x	x	x
AVERROES	x	x			x	x	
CRETIN	x	x	x	x	x	x	x
CRETINL	x	x	x	x	x	x	x
ECRSS	x	x	x				
FAC						x	
FLYCHK	x	x	x	x	x	x	x
GONDOR					x	x	
HULLAC v.9	x				x		
JATOM	x		x	x	x	x	
MOST/AVE					x		
NOHEL					x	x	
NOHEL2E					x	x	
NOMAD	x	x					x
RADIOM					x	x	
SCAALP					x	x	
SCRAM	x	x	x	x			
SCRIC	x	x				x	
SCROLL		x			x	x	
THERMOS	x	x	x	x	x	x	
XSTAR			x				

Figure 6. List of contributions and participant codes of NLTE-4 Workshop

It has been observed a good agreement of atomic and radiative properties with respect to results of other codes which have participated in the storage inside the 4th NLTE database [18]. Iron plasmas at so low a density can't be managed with ATMED CR.

.

References

[1] A.J. Benita, E. Mínguez, M.A. Mendoza, J.G. Rubiano, J.M. Gil, R. Rodríguez, P. Martel. Collisional Radiative Average Atom Code Based on a Relativistic Screened Hydrogenic Model. High Energy Density Physics 14 (2015) 18-29.

[2] A.J. Benita. Collisional Radiative Average Atom Code With Relativistic Atomic Model. Theoretical physics. ISBN: 978-620-2-01943-9. LAP Lambert Academic Publishing (2017).

[3] A.J. Benita. Fast Calculation of Plasmas Properties with ATMED LTE. Project of Nuclear Science and Technology Master at UPM (2012).

[4] M.A. Mendoza, J.G. Rubiano, J.M. Gil, R. Rodriguez, R. Florido, A.J. Benita, P. Martel, E. Minguez. Fast Computation of Radiative Properties and EOS of Warm Dense Matter using the ATMED code. Eight International Conference on Inertial Fusion Sciences and Applications (IFSA 2013). September 8 -13 (2013) Nara, Japan.

[5] M.A. Mendoza, J.G. Rubiano, J.M. Gil, R. Rodriguez, R. Florido, G. Espinosa, P. Martel, E. Minguez. Calculation of radiative opacity of plasma mixtures using a relativistic screened hydrogenic model. Journal of Quantitative Spectroscopy & Radiative Transfer 140 (2014) 81–98.

[6] M.A. Mendoza, J.G. Rubiano, J.M. Gil, R. Rodriguez, R. Florido, P. Martel, E. Minguez. A new set of relativistic screening constants for the screened hydrogenic model. HEDP 7 (2011) 169–179.

[7] F.H. Ruano, J.G. Rubiano, M.A. Mendoza, J.M.Gil, R. Rodriguez, R. Florido, P. Martel, E. Minguez. Relativistic screened hydrogenic radial integrals. Journal of Quantitative Spectroscopy & Radiative Transfer (2012) 117123-132.

[8] W.A. Lokke and W.H. Grasberger. XSNQ-U A Non-LTE Emission and Absorption Coefficient Subroutine. Prepared for U.S. Energy Research & Development Administration under contract No. W-7405-Eng-48, UCRL-52276 (1977).

[9] Joseph Abdallah et al. The reduced detailed configuration accounting (RDCA) model for NLTE plasma calculations. High Energy Density Physics 4 (2008) 124–130.

[10] G.Faussurier, C. Blancard, T. Kato, R. M. More. Prigogine theorem of minimum entropy production applied to the average atom model. High Energy Density Physics 5 (2009) 283–293.

[11] G.Faussurier et al. Nonlocal thermodynamic equilibrium self-consistent average-atom model for plasma physics. PHYSICAL REVIEW E, VOLUME 63, 026401 (2001).

[12] Balazs F. Rozsnyai. Collisional radiative average atom model for hot plasmas. Physical Review E 55, (1996).

[13] Balazs F. Rozsnyai. Hot plasma opacities in the presence or absence of local thermodynamic equilibrium. High Energy Density Physics 6 (2010) 345–355.

[14] A.F. Nikiforov, V.G. Novikov, V.B. Uvarov. Quantum-statistical models of hot dense matter. Methods for Computation Opacity and Equation of State. Birkhäuser Verlag (2005).

[15] A.J. Benita. Calculation of Temporal Plasmas of XFEL Experiments with a Relativistic Collisional Radiative Average Atom Code. Physical Science International Journal, DOI: 10.9734/PSIJ/2018/40246 (2018).

[16] A.J. Benita. Book Summary ISBN 978-620-2-01943-9. https://www.researchgate.net/profile/Aj_Benita (2017).

[17] A.J. Benita. Comparison of Iron Plasma Atomic and Radiative Properties Computed with a Relativistic Collisional Radiative Average Atom Code versus Other Models. Asian Journal of Research and Reviews in Physics, DOI: 10.9734/AJR2P/2018/41729 (2018).

[18] https://nlte.nist.gov/NLTE4/

[19] J.G. Rubiano et al. Review of the 4th NLTE Code Comparison Workshop. High Energy Density Physics 3 (2007) 225-232.

[20] J.G. Rubiano et al. The 4th Non-LTE Code Comparison Workshop. Submission of Calculations. December 12-16, (2005).

[21] Z.Q. Wu, B. Duan, J. Yan. Effects of different doubly excited states on the ionization balance and M-emissivity in high-Z plasmas. High Energy Density Physics 11 (2014) 70–74.

[22] H.-K. Chung et al. FLYCHK : Generalized population kinetics and spectral model for rapid spectroscopic analysis for all elements. UCRL-JRNL-213347. High Energy Density Physics (2005).

[23] H.A. Scott and S.B. Hansen. Advances in NLTE modeling for integrated simulations. High Energy Density Physics 6 (2010) 39–47.